




Cite this: *Polym. Chem.*, 2025, **16**, 569

# Aziridine-based organocatalytic polymerization for tunable sulfur incorporation in polyureas†

Leying Xu,<sup>a</sup> Changzheng Ju,<sup>a</sup> Jiazi Zheng,<sup>a</sup> Qingyong Chen<sup>a</sup> and Zhen Zhang  <sup>a,b</sup>

Developing new methods for converting inorganic sulfur into sulfur-containing polymers is crucial for advancing both sustainable development and innovative polymeric materials. In this study, we present an aziridine-based polymerization strategy to synthesize polyureas with tunable sulfur incorporation. The process begins with the reaction of aziridine with isocyanate, followed by a ring-opening reaction with an inorganic sulfur reagent. When elemental sulfur is used, oligosulfide anions form in the presence of an organobase, which then nucleophilically attack the aziridine ring, producing oligosulfide-functionalized polyureas. Alternatively, using sodium sulfide generates poly(thioether urea)s through a similar ring-opening mechanism. Model reactions confirm successful sulfur incorporation during these processes. Additionally, a cross-linked polyurea synthesized with tri-isocyanate exhibits excellent mechanical properties, with tensile stress exceeding 30 MPa, and demonstrates good reprocessability due to the dynamic nature of the oligosulfide bonds. Overall, this polymerization approach broadens the range of sulfur-containing materials and supports further advances in aziridine-based polymer chemistry.

Received 20th October 2024,  
Accepted 19th December 2024

DOI: 10.1039/d4py01171f

rsc.li/polymers

## Introduction

Sulfur, a byproduct of the oil and gas industry, is generated during fossil fuel refining processes where sulfur compounds are removed to reduce pollution and meet environmental standards.<sup>1</sup> Despite its essential roles in producing sulfuric acid, rubber vulcanization, and fertilizers, sulfur production consistently exceeds demand.<sup>2</sup> Consequently, there is a growing need to find innovative ways to convert sulfur byproducts into economically viable and environmentally sustainable products.<sup>3</sup>

One promising approach is the conversion of sulfur compounds into sulfur-containing polymers, which possess unique chemical properties and potential applications in fields such as energy storage, optics, adhesives, and environmental remediation.<sup>4–8</sup> The versatile chemistry of sulfur allows for the formation of various bond types, including C–S, C=S, and polysulfide (–S<sub>x</sub>–) linkages. For example, C–S bonds are utilized in the synthesis of poly(thioethers) through copolymerization of carbon disulfide with epoxides,<sup>9</sup> or by step-growth polymerization of H<sub>2</sub>S with diacrylates.<sup>10</sup> Numerous polymerization strategies have been developed for synthesizing polythioamides<sup>11–15</sup> and polythioureas<sup>16–18</sup> using elemental

sulfur to form C=S bonds. Inverse vulcanization, where elemental sulfur is copolymerized with organic crosslinkers, has emerged as a particularly promising method for creating sulfur-rich polymers featuring oligosulfide linkages.<sup>19–24</sup> These dynamic, reversible linkages can impart self-healing, recyclable, and reprocessable properties to materials.<sup>25,26</sup> However, inverse vulcanization typically yields cross-linked structures, and synthesizing linear polymers with controlled sulfur incorporation remains challenging.

Recent advancements have enabled the production of tunable sulfur-incorporated polymers. Pyun *et al.*, for instance, utilized sulfur monochloride (S<sub>2</sub>Cl<sub>2</sub>) to polymerize with allylic monomers, producing linear polyhalodisulfides.<sup>27</sup> Similarly, Ren *et al.* polymerized S<sub>8</sub> with episulfides, generating polydisulfides and copolymers with distinct disulfide and polysulfide segments by employing different organocatalysts.<sup>28</sup> More recently, we developed a step-growth polymerization of bis(*N*-sulfonyl/carbonyl aziridines) with elemental sulfur, yielding linear polysulfides through ring-opening reactions involving oligosulfide anions.<sup>29</sup>

Aziridines have long been studied in polymer chemistry.<sup>30,31</sup> Anionic ring-opening polymerization of *N*-sulfonyl aziridines, activated by *N*-electron-withdrawing groups, has garnered attention due to its ability to generate well-defined poly(*N*-sulfonyl aziridine)s.<sup>32–37</sup> In contrast, *N*-unsubstituted aziridines, such as ethyleneimine and propyleneimine, are widely used industrially.<sup>38</sup> The cationic ring-opening polymerization of these *N*-unsubstituted aziridines is the predominant method for producing polyethyleneimine

<sup>a</sup>School of Chemical Engineering and Light Industry, Guangdong University of Technology, Guangzhou 510006, China. E-mail: zhen.zhang@gdut.edu.cn

<sup>b</sup>Jieyang Branch of Chemistry and Chemical Engineering Guangdong Laboratory (Rongjiang Laboratory), Jieyang 515200, China

† Electronic supplementary information (ESI) available. See DOI: <https://doi.org/10.1039/d4py01171f>

and its derivatives. Though some copolymerizations of *N*-unsubstituted aziridines with CO<sub>2</sub>,<sup>39</sup> COS,<sup>40</sup> or tosyl isocyanate<sup>41</sup> have been reported, new polymerization approaches using *N*-unsubstituted aziridines remain largely unexplored.

In this study, we present an organocatalytic step-growth polymerization approach using *N*-unsubstituted aziridines to introduce tunable sulfur incorporation in polyureas. This versatile approach enables the efficient production of sulfur-containing polymers. Aziridines, such as 2-methylaziridine and 2-benzylaziridine, first react with diisocyanates, followed by sulfur incorporation using either elemental sulfur or sodium sulfide, resulting in the formation of oligosulfide or thioether linkages within the polymer backbone. We successfully synthesized 14 distinct polyureas and a cross-linked poly(urea sulfide) vitrimer. This efficient cascade process offers a valuable platform for producing novel sulfur-containing polymers.

## Results and discussion

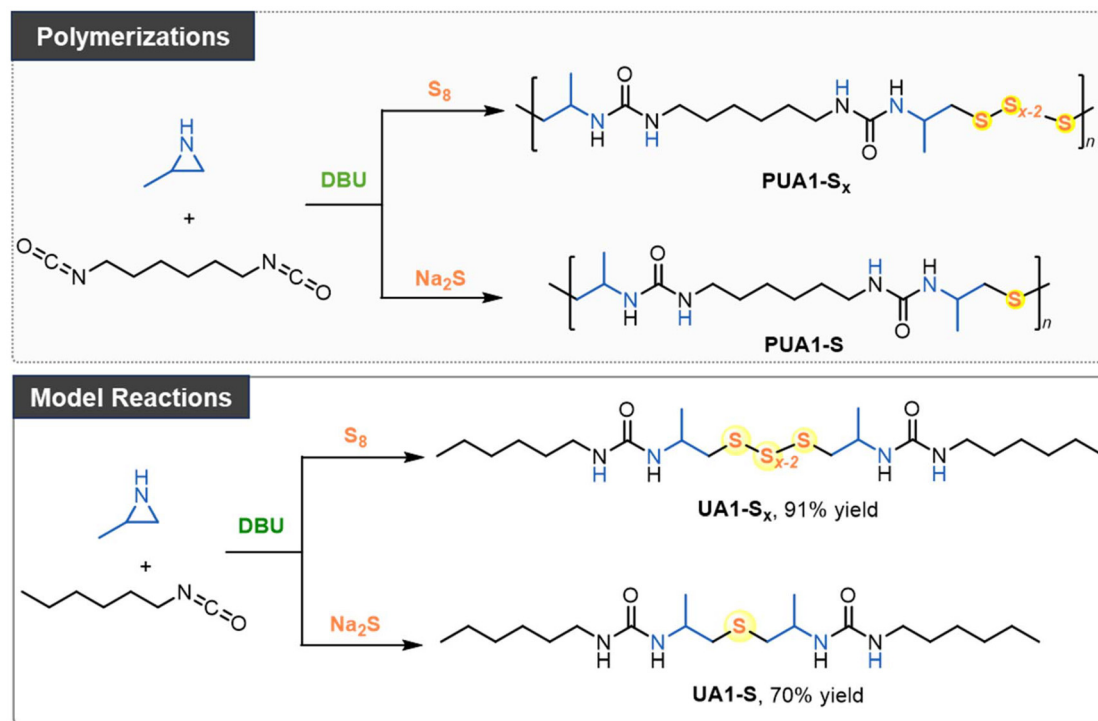
### Polymerizations of aziridine, isocyanate, and inorganic sulfur

*N*-Tosyl aziridines have been shown to react with sulfur reagents, such as tetrathiomolybdate<sup>42</sup> and sodium disulfide,<sup>43</sup> to form  $\beta$ -sulfonamidodisulfides. However, the limited availability of these sulfur transfer reagents constrains their broader application. Recently, we found that elemental sulfur can react with bis(*N*-tosyl/carbonyl aziridines) in the presence of an organobase, leading to the formation of linear polysulfides.<sup>29</sup> Building on this, and given that 2-methylaziridine

readily reacts with isocyanates, as shown in our previous alternating copolymerization studies,<sup>41</sup> we proposed a new pathway for the polymerization of aziridine, isocyanate, and elemental sulfur (Scheme 1).

In the initial experiments (Table S1†), 1,6-diisocyanatohexane (1.0 equiv.), 2-methylaziridine (2.0 equiv.), and elemental sulfur (4.0 equiv.) were polymerized in DMSO using MTBD (10 mol%) as the organocatalyst to transfer elemental sulfur into oligosulfide anions. After 36 hours of stirring, the reaction was terminated by adding the mixture to a large excess of methanol, and the resulting precipitate was analyzed by SEC and NMR. SEC analysis revealed that the resulting oligomer had a number-average molecular weight ( $M_{n,SEC}$ ) of 3270 Da with a dispersity of 1.20. NMR confirmed the successful incorporation of both isocyanate and aziridine monomers into the polymer chain, though the exact chemical structure remained undetermined. Further screening of polymerization conditions revealed that using other organic superbases, such as *t*-BuP<sub>4</sub>, and solvents did not increase the molar mass (Table S1†). However, reducing the amount of elemental sulfur to 2.0 equivalents increased the molar mass to 6050 Da, with a dispersity of 2.08. In contrast, increasing the sulfur amount to 8.0 equivalents resulted in a lower molar mass of 3250 Da, similar to that obtained with 4.0 equivalents of sulfur. These results demonstrate that the amount of sulfur significantly influences polymerization.

Polymerization with 2.0 equiv. of sulfur in DMSO at 100 °C, using various catalysts, showed that DBU, MTBD, and *t*-BuP<sub>2</sub> produced polymers with  $M_{n,SEC}$  values ranging from 14.1 to



**Scheme 1** Polymerizations and model reactions of aziridine, isocyanate, and inorganic sulfur.

16.2 kDa, with dispersities exceeding 2.5 (Table S2†). In contrast, PMDETA and *t*-BuP<sub>4</sub> produced polymers with lower molar masses. DBU was then selected as the catalyst, and a larger-scale (0.5 mmol of 1,6-diisocyanatohexane) polymerization yielded a polymer with a molar mass exceeding 10 kDa. Notably, the polymerization proceeded smoothly even when water (10.0 equiv.) was added to the mixture, still yielding the desired polymer. Reducing the reaction temperature to 40 °C or decreasing the catalyst loading to 5 mol% led to lower  $M_{n,SEC}$  values as determined by SEC.

Inspired by the reaction between aziridine and sodium disulfide,<sup>43</sup> we also explored incorporating sulfur using sulfide salts (Table S3†). Replacing elemental sulfur with sodium sulfide in the polymerization, and using DBU as the catalyst in DMSO, produced a polymer with a molar mass of 6440 Da and a dispersity of 1.87 after 18 hours at 100 °C. Lowering the reaction temperature to 70 °C and 40 °C increased the molar masses to 10.88 and 8.61 kDa, respectively. It should be noted that no polymerization occurred in the absence of a catalyst. Reducing the catalyst loading to 5 mol% resulted in a lower  $M_{n,SEC}$  value.

### Model reactions and polymer structural characterizations

We hypothesize that when using elemental sulfur, oligosulfides are incorporated into the polymer, whereas thioethers are generated when sodium sulfide is used as the sulfur transfer reagent. To clarify the polymer structures, reaction pathways, and mechanisms, we conducted model reactions involving 2-methylaziridine, hexyl isocyanate, and inorganic sulfur (Scheme 1).

Initially, 2-methylaziridine (1.0 equiv.) was treated with hexyl isocyanate (1.0 equiv.) in DMSO, followed by the addition of elemental sulfur (5.0 equiv.) and DBU (10 mol%). The mixture was sealed and stirred at 100 °C for 12 hours. Water was then added to remove any unreacted salt, and the product was extracted with dichloromethane. The organic phase was

evaporated, yielding a brown solid, which was directly analyzed by NMR and MS without further purification. The product is presumed to contain two urea moieties linked by polysulfide bonds. <sup>1</sup>H NMR confirmed the ring-opening of the aziridine, with characteristic signals for aliphatic protons from both the aziridine and hexyl isocyanate (Fig. 1a). The <sup>13</sup>C NMR spectrum showed multiple peaks for carbon atoms (–CH<sub>2</sub>–S<sub>x</sub>–CH<sub>2</sub>–), corresponding to varying sulfur lengths. MS analysis further supported the presence of sulfur ranks ranging from 2 to 5 atoms (Fig. 2a). Importantly, the peaks in the <sup>1</sup>H and <sup>13</sup>C NMR spectra of the polymer closely matched those of the model compound, confirming that the polymer backbone includes a polydisulfide moiety (Fig. 1a and Fig. S1†). Additionally, DEPT 135° analysis further validated the desired structure (Fig. S2†).

Next, we performed a reaction with 2-methylaziridine (1.0 equiv.), hexyl isocyanate (1.0 equiv.), and sodium sulfide (1.5 equiv.) in DMSO at 100 °C, using DBU (10 mol%) as the catalyst. Water was then added, and the product was isolated through dichloromethane extraction. The <sup>1</sup>H NMR spectrum displayed characteristic signals for aliphatic protons similar to those observed in the oligosulfide product (UA1-S<sub>x</sub>), except for the –CH<sub>2</sub>–S–CH<sub>2</sub>– peaks at 2.43–2.48 ppm. The <sup>13</sup>C NMR spectrum showed sulfur-linked carbon atoms at 47.2 ppm, compared to the multiple peaks at around 46 ppm observed for UA1-S<sub>x</sub>. HRMS analysis confirmed the presence of a thioether moiety, as evidenced by the observed species at [M + H]<sup>+</sup> 403.30978 and [2M – H]<sup>+</sup> 805.61224 in the spectrum (Fig. 2b). Based on the NMR spectra comparison between the model compound and the polymer (Fig. 1b and Fig. S3†), we conclude that the polymer derived from sodium sulfide contains both thioether and urea moieties within its repeating units. FT-IR analysis of the polymers further confirmed the presence of the C=O, C–S, and N–H groups in the polymer backbone (Fig. S4†).

Based on the literature and our experimental results,<sup>44,45</sup> we propose a mechanism for the cascade reactions (Scheme 2).

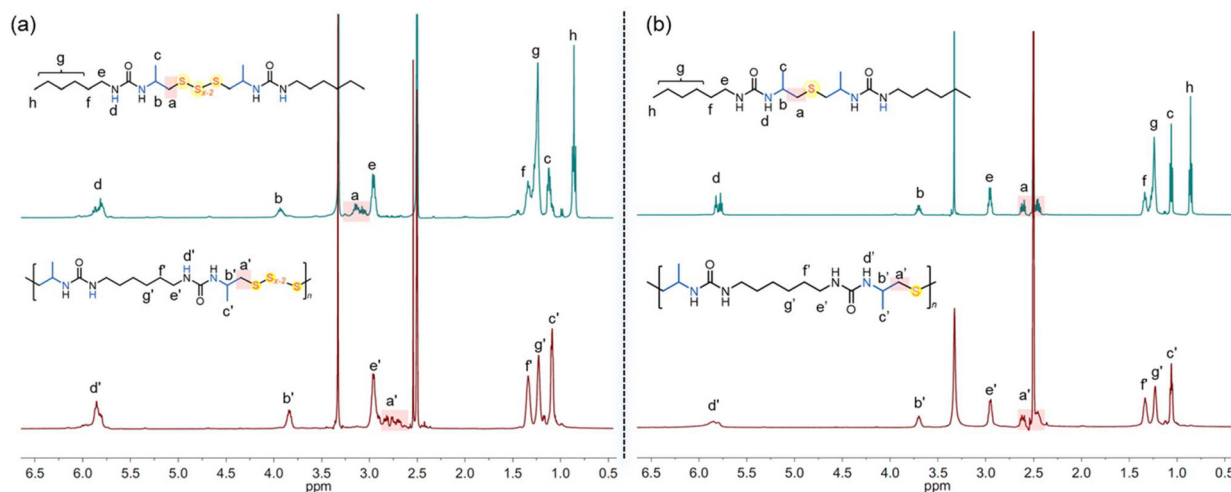


Fig. 1 <sup>1</sup>H NMR spectra of (a) UA1-S<sub>x</sub> and PUA1-S<sub>x</sub>, and (b) UA1-S and PUA1-S.

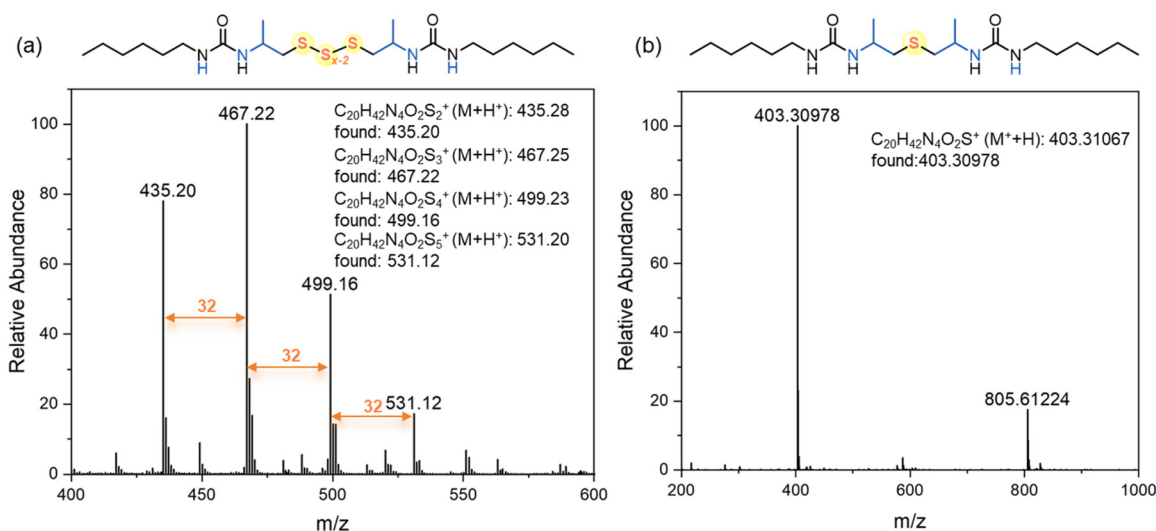
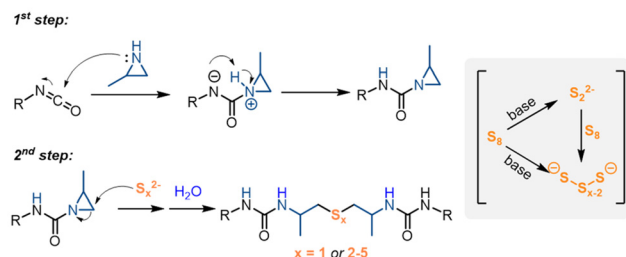


Fig. 2 (a) APCI MS spectrum of UA1-S<sub>x</sub>, and (b) HRMS spectrum of UA1-S.



Scheme 2 A proposed mechanism for the cascade reaction.

The process begins with a nucleophilic attack of the aziridine on the isocyanate, forming an aziridine-1-carboxamide intermediate. Organobase-mediated cleavage of the octasulfur ring generates polysulfide anions of varying chain lengths, which may further react with sulfur to produce additional polysulfide anions.<sup>44</sup> These polysulfide anions then undergo nucleophilic addition to the less-substituted carbon of the aziridine ring, forming urea anions. A proton transfer from water completes the formation of the desired urea. In reactions with sodium sulfide, the organobase probably stabilizes the sulfide anions, facilitating their nucleophilic addition to the aziridine rings.

### Monomer scopes

After establishing the optimized polymerization conditions, we proceeded to evaluate the applicability of various monomers, as summarized in Table 1. Aliphatic and aromatic diisocyanates (**1b–1e**) were polymerized smoothly with aziridine **2a** and elemental sulfur, yielding the desired polymers (PUA2-S<sub>x</sub> to PUA5-S<sub>x</sub>) in 75–97% yield, with molar masses ( $M_{n,SEC}$ ) ranging from 5.65 to 14.66 kDa under the optimized conditions (entries 2–5, Table 1). Next, 2-benzylaziridine (**2b**) was used in place of **2a**, successfully producing polyureas PUA6-S<sub>x</sub> and PUA7-S<sub>x</sub> with molar masses of 15.49 and 13.09 kDa, and

yields of 77% and 73%, respectively (entries 6 and 7, Table 1). The synthesized PUA-S<sub>x</sub> samples were analyzed using organic elemental analysis (OEA), and the experimental sulfur content closely matched the theoretical values (entries 1–7, Table 1 and Table S4†). This indicates that the elemental sulfur from the feed was successfully incorporated into the polymers.

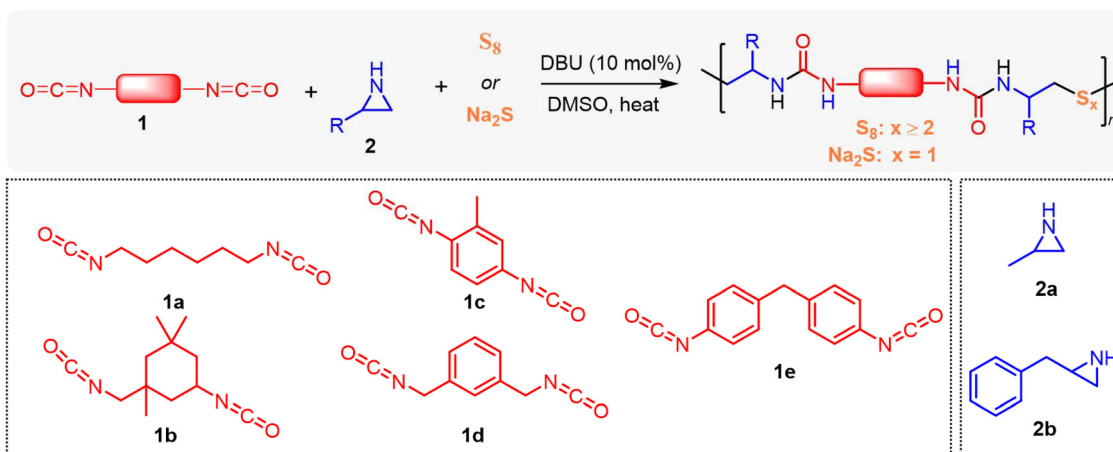
When sodium sulfide was employed instead of elemental sulfur, the corresponding poly(thioether urea)s PUA2-S to PUA7-S were obtained in 61–89% yield, with molar masses ranging from 5.62 to 28.27 kDa (entries 9–14, Table 1). The SEC traces of oligosulfide-functionalized polyureas (PUA1-S<sub>x</sub> to PUA7-S<sub>x</sub>) are shown in Fig. 3a, while those for poly(thioether urea)s (PUA1-S to PUA7-S) are shown in Fig. 3b. X-ray diffraction (XRD) patterns (Fig. S5 and S6†) showed that neither of the synthesized polymers, PUA1-S<sub>x</sub> nor PUA1-S, contained residual crystalline sulfur or sodium sulfide. Additionally, scanning electron microscopy (SEM) and elemental mapping (Fig. S7 and S8†) confirmed that the elemental distribution in the polymer films was uniform.

### Thermal properties

The thermal characteristics of polyureas were analyzed using thermogravimetric analysis (TGA) and differential scanning calorimetry (DSC). The polysulfides demonstrated relatively limited thermal resistance, as indicated by their lower decomposition temperatures ( $T_{d,5\%}$ ), occurring below 236 °C (Fig. 3c) under a nitrogen atmosphere. In contrast, the corresponding poly(thioether urea)s exhibited a slightly higher decomposition temperature, reaching up to 277 °C (Fig. 3d). This suggests that the thioether segments are more stable than the –S–S– bonds.

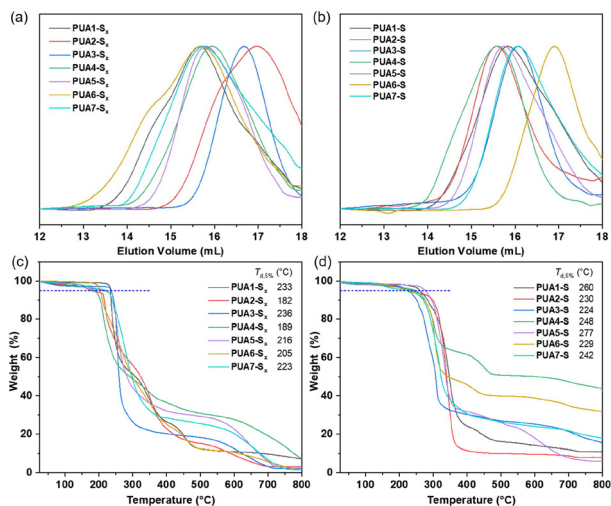
DSC analysis in Fig. S9 and S10† revealed that the glass transition temperatures ( $T_g$ ) of polyureas derived from diisocyanate **1a**, which incorporated softer aliphatic segments, ranged from 48 to 87 °C. In contrast, polyureas containing



**Table 1** Synthesis of polyureas through organocatalytic polymerization of aziridine, isocyanate, and inorganic sulfur

| Entry <sup>a</sup> | Polymer             | Monomers                | Time (h) | $M_{n,SEC}$ <sup>b</sup> (kDa) | $M_{w,SEC}$ <sup>b</sup> (kDa) | $D$ <sup>b</sup> | Sulfur content (wt%) |                   | Yield <sup>e</sup> (%) | $T_g$ <sup>f</sup> (°C) | $T_{d,5\%}$ <sup>g</sup> (°C) |
|--------------------|---------------------|-------------------------|----------|--------------------------------|--------------------------------|------------------|----------------------|-------------------|------------------------|-------------------------|-------------------------------|
|                    |                     |                         |          |                                |                                |                  | Theor. <sup>c</sup>  | Exp. <sup>d</sup> |                        |                         |                               |
| 1                  | PUA1-S <sub>x</sub> | 1a/2a/S <sub>8</sub>    | 24       | 16.2                           | 47.3                           | 2.92             | 17.7                 | 19.4              | 91                     | 82                      | 233                           |
| 2                  | PUA2-S <sub>x</sub> | 1b/2a/S <sub>8</sub>    | 24       | 5.6                            | 11.8                           | 2.09             | 15.9                 | 16.2              | 88                     | —                       | 182                           |
| 3                  | PUA3-S <sub>x</sub> | 1c/2a/S <sub>8</sub>    | 24       | 8.2                            | 11.9                           | 1.46             | 18.1                 | 17.4              | 97                     | —                       | 236                           |
| 4                  | PUA4-S <sub>x</sub> | 1d/2a/S <sub>8</sub>    | 22       | 12.4                           | 29.2                           | 2.35             | 17.4                 | 18.9              | 75                     | 72                      | 189                           |
| 5                  | PUA5-S <sub>x</sub> | 1e/2a/S <sub>8</sub>    | 24       | 14.7                           | 27.4                           | 1.87             | 14.9                 | 16.4              | 93                     | —                       | 216                           |
| 6                  | PUA6-S <sub>x</sub> | 1a/2b/S <sub>8</sub>    | 12       | 15.5                           | 67.0                           | 4.33             | 15.0                 | 16.7              | 77                     | 48                      | 205                           |
| 7                  | PUA7-S <sub>x</sub> | 1e/2b/S <sub>8</sub>    | 24       | 13.1                           | 33.6                           | 2.57             | 12.8                 | 14.7              | 73                     | —                       | 223                           |
| 8                  | PUA1-S              | 1a/2a/Na <sub>2</sub> S | 18       | 10.9                           | 27.6                           | 2.54             | —                    | —                 | 77                     | 87                      | 260                           |
| 9                  | PUA2-S              | 1b/2a/Na <sub>2</sub> S | 18       | 16.6                           | 33.9                           | 2.05             | —                    | —                 | 69                     | —                       | 230                           |
| 10                 | PUA3-S              | 1c/2a/Na <sub>2</sub> S | 18       | 15.3                           | 23.3                           | 1.53             | —                    | —                 | 83                     | —                       | 224                           |
| 11                 | PUA4-S              | 1d/2a/Na <sub>2</sub> S | 18       | 28.3                           | 49.4                           | 1.75             | —                    | —                 | 89                     | 113                     | 248                           |
| 12                 | PUA5-S              | 1e/2a/Na <sub>2</sub> S | 18       | 14.3                           | 27.8                           | 1.95             | —                    | —                 | 72                     | —                       | 277                           |
| 13                 | PUA6-S              | 1a/2b/Na <sub>2</sub> S | 18       | 5.6                            | 8.8                            | 1.57             | —                    | —                 | 62                     | 61                      | 229                           |
| 14                 | PUA7-S              | 1e/2b/Na <sub>2</sub> S | 12       | 9.4                            | 19.0                           | 2.04             | —                    | —                 | 61                     | 150                     | 242                           |

<sup>a</sup> Reaction conditions: for entries 1–7,  $[1]_0/[2]_0/[S_8]_0/[DBU]_0 = 1/2/2/0.1$ , DMSO, 100 °C; for entries 8–14,  $[1]_0/[2]_0/[Na_2S]_0/[DBU]_0 = 1/2/3/0.1$ , DMSO, 70 °C. <sup>b</sup> Determined by SEC in DMF at 60 °C (PMMA standard calibration). <sup>c</sup> Theoretical weight ratio (wt%) of sulfur. <sup>d</sup> Experimental weight ratio (wt%) of sulfur, determined by organic elemental analysis (OEA). <sup>e</sup> Isolated yield. <sup>f</sup>  $T_g$  is the glass transition temperature. <sup>g</sup>  $T_{d,5\%}$  is the initial decomposition temperature at 5% weight loss measured under a nitrogen atmosphere.

**Fig. 3** SEC traces of (a) PUA-S<sub>x</sub>, and (b) PUA-S. TG curves of (c) PUA-S<sub>x</sub>, and (d) PUA-S.

rigid aryl moieties, such as PUA7-S derived from **1e**, exhibited higher  $T_g$  values at 150 °C. Notably, endothermic melting peaks at 112 °C and 62 °C were observed in the DSC curves for samples PUA1-S<sub>x</sub> and PUA7-S<sub>x</sub>, respectively, indicating the presence of crystalline structures in these two polymers. Corresponding exothermic crystallization peaks were also noted in the cooling curves for both samples (Fig. S9†).

### Polyurea vitrimer synthesis

Vitrimers, a class of cross-linked polymer materials that integrate the durability of thermosets with the reprocessability of thermoplastics, have garnered significant research attention in recent years.<sup>46–48</sup> Their dynamic covalent network allows for excellent thermal stability, recyclability, and mechanical robustness. Based on the established polymerization reactions, we aimed to synthesize polyurea vitrimers, where the dynamic behavior is driven by exchange reactions within the oligosulfide segments. These reactions occur through a reversible bond exchange mechanism, allowing the network to rearrange

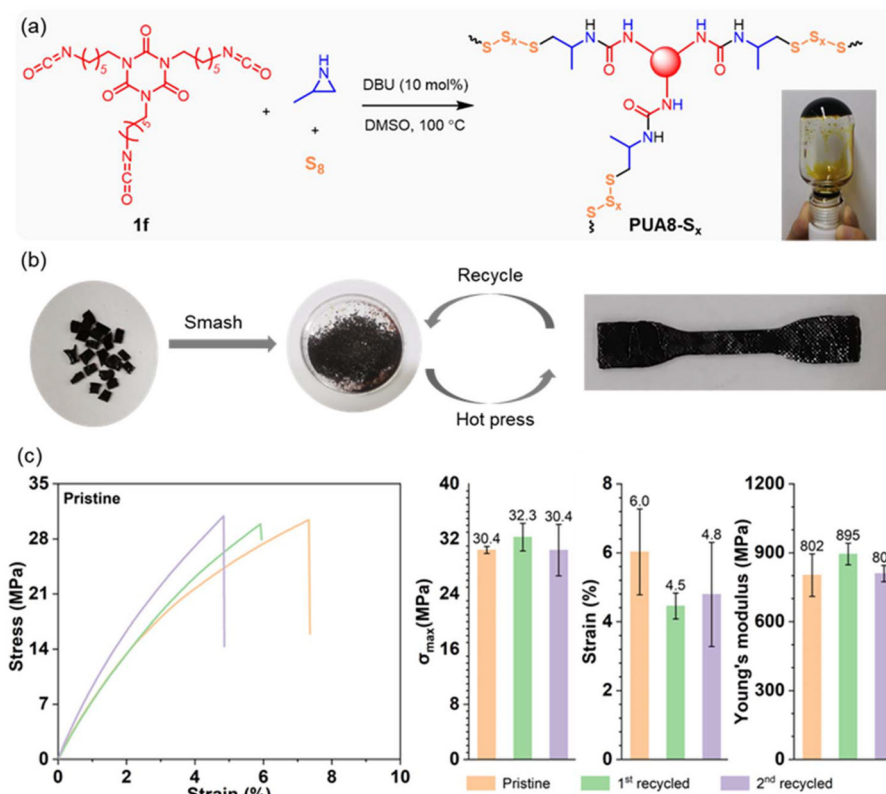


**Fig. 4** (a) Synthesis of polyurea vitrimer PUA8-S<sub>x</sub>. (b) The recycling process for the polyurea vitrimer sheet. (c) Stress–strain curves, maximum stress, breaking strain, and Young's modulus of vitrimer PUA8-S<sub>x</sub> before recycling and after two recycling cycles.

or reshape under heat. The polymerization was carried out in DMSO using tri-isocyanate **1f**, aziridine **2a**, and elemental sulfur as monomers, with DBU as the catalyst (Fig. 4a). After heating at 100 °C for 1 hour, a gel was formed, indicating successful cross-linking. The gel was then dried under vacuum, ground into a powder, and then hot-pressed into a dog-bone-shaped sheet (Fig. 4b). This vitrimer exhibited a  $T_{d,5\%}$  of 231 °C, and a  $T_g$  of 75 °C (Fig. S11†).

The mechanical properties of the resulting vitrimer sheet were evaluated through stress–strain testing. The vitrimer demonstrated high mechanical strength, with a maximum stress of  $30.4 \pm 0.5$  MPa and Young's modulus of  $802 \pm 93$  MPa (Fig. 4c). After testing, the sheet was recycled by grinding it into a powder and reshaping it *via* hot pressing at 140 °C and 10 MPa for 5–10 minutes (Fig. 4b), showcasing excellent reprocessability. Following two recycling cycles (Fig. S12†), the maximum stress remained above 30 MPa, while Young's modulus was over 800 MPa. These results confirm the good recyclability and mechanical performance of the polysulfide-based vitrimer synthesized in this study.

The polymerization of tri-isocyanate **1f**, aziridine **2a**, and sodium sulfide was also conducted, resulting in the formation of a gel, which was subsequently dried (Fig. S13†). We attempted to prepare dog-bone-shaped samples by hot-pressing; however, as anticipated, the reprocessing of this cross-linked polymer was

unsuccessful. By comparing this material to PUA8-S<sub>x</sub>, which incorporates oligosulfide segments, we can conclude that the dynamic sulfur exchange in the oligosulfide segments (–S<sub>x</sub>–) contributes to the material's dynamic behavior.

## Conclusions

In conclusion, this study presents a successful polymerization approach for synthesizing sulfur-containing polyureas with tunable sulfur incorporation, using aziridine, isocyanates, and inorganic sulfur reagents. The approach yields oligosulfide-functionalized polyureas or poly(thioether urea)s depending on the sulfur source. Additionally, the synthesis of a cross-linked polyurea demonstrates excellent mechanical strength and reprocessability, offering a promising avenue for developing advanced, sustainable polymeric materials. This work broadens the scope of sulfur-containing polymers and highlights the potential of aziridine-based polymerization.

## Data availability

The data supporting this article have been included as part of the ESI.†

## Conflicts of interest

There are no conflicts to declare.

## Acknowledgements

This work is financially supported by the National Natural Science Foundation of China (22378080), and Guangdong Basic and Applied Basic Research Foundation (2023A1515030156).

## References

- 1 D. A. Boyd, *Angew. Chem., Int. Ed.*, 2016, **55**, 15486–15502.
- 2 R. Priyadarshi, A. Khan, P. Ezati, S. K. Tammina, S. Priyadarshi, T. Bhattacharya, J. T. Kim and J.-W. Rhim, *Environ. Chem. Lett.*, 2023, **21**, 1673–1699.
- 3 J. Lim, J. Pyun and K. Char, *Angew. Chem., Int. Ed.*, 2015, **54**, 3249–3258.
- 4 J. J. Griebel, R. S. Glass, K. Char and J. Pyun, *Prog. Polym. Sci.*, 2016, **58**, 90–125.
- 5 H. Mutlu, E. B. Ceper, X. Li, J. Yang, W. Dong, M. M. Ozmen and P. Theato, *Macromol. Rapid Commun.*, 2019, **40**, 1800650.
- 6 Y. Zhang, R. S. Glass, K. Char and J. Pyun, *Polym. Chem.*, 2019, **10**, 4078–4105.
- 7 N. P. Tarasova, A. A. Zanin, E. G. Krivoborodov and Y. O. Mezhev, *RSC Adv.*, 2021, **11**, 9008–9020.
- 8 T. Lee, P. T. Dirlam, J. T. Njardarson, R. S. Glass and J. Pyun, *J. Am. Chem. Soc.*, 2022, **144**, 5–22.
- 9 C.-J. Zhang and X.-H. Zhang, *Macromolecules*, 2020, **53**, 233–239.
- 10 Z. Liu, Y. Xia, W. Guo, C. Zhang and X. Zhang, *Macromol. Chem. Phys.*, 2024, **225**, 2300449.
- 11 G. Guo, J. Sun, C. Zhao, Y. Liu and C.-M. Liu, *Green Chem.*, 2016, **18**, 1278–1286.
- 12 W. Li, X. Wu, Z. Zhao, A. Qin, R. Hu and B. Z. Tang, *Macromolecules*, 2015, **48**, 7747–7754.
- 13 L. Zhang, Y. Hu, R. Hu and B. Z. Tang, *Chem. Commun.*, 2022, **58**, 1994–1997.
- 14 Y. Huang, R. Hu and B. Z. Tang, *Macromolecules*, 2024, **57**, 6568–6576.
- 15 W. Cao, F. Dai, R. Hu and B. Z. Tang, *J. Am. Chem. Soc.*, 2020, **142**, 978–986.
- 16 T. Tian, R. Hu and B. Z. Tang, *J. Am. Chem. Soc.*, 2018, **140**, 6156–6163.
- 17 N. Zheng, H. Gao, Z. Jiang and W. Song, *Sci. China: Chem.*, 2023, **66**, 870–877.
- 18 Y. Huang, Y. Yu, R. Hu and B. Z. Tang, *J. Am. Chem. Soc.*, 2024, **146**, 14685–14696.
- 19 W. J. Chung, J. J. Griebel, E. T. Kim, H. Yoon, A. G. Simmonds, H. J. Ji, P. T. Dirlam, R. S. Glass, J. J. Wie, N. A. Nguyen, B. W. Guralnick, J. Park, Á. Somogyi, P. Theato, M. E. Mackay, Y.-E. Sung, K. Char and J. Pyun, *Nat. Chem.*, 2013, **5**, 518–524.
- 20 K. S. Kang, A. Phan, C. Olikagu, T. Lee, D. A. Loy, M. Kwon, H. J. Paik, S. J. Hong, J. Bang and W. O. Parker Jr, *Angew. Chem., Int. Ed.*, 2021, **60**, 22900–22907.
- 21 D. Wang, Z. Tang, Z. Wang, L. Zhang and B. Guo, *Polym. Chem.*, 2022, **13**, 485–491.
- 22 X. Wu, J. A. Smith, S. Petcher, B. Zhang, D. J. Parker, J. M. Griffin and T. Hasell, *Nat. Commun.*, 2019, **10**, 647.
- 23 P. Yan, W. Zhao, B. Zhang, L. Jiang, S. Petcher, J. A. Smith, D. J. Parker, A. I. Cooper, J. Lei and T. Hasell, *Angew. Chem., Int. Ed.*, 2020, **59**, 13371–13378.
- 24 J. M. Scheiger, M. Hoffmann, P. Falkenstein, Z. Wang, M. Rutschmann, V. W. Scheiger, A. Grimm, K. Urbschat, T. Sengpiel, J. Matysik, M. Wilhelm, P. A. Levkin and P. Theato, *Angew. Chem., Int. Ed.*, 2022, **61**, e202114896.
- 25 Y. Zhang, F. Seidi, M. Ahmad, L. Zheng, L. Cheng, Y. Huang and H. Xiao, *Green Chem.*, 2023, **25**, 6515–6537.
- 26 R. Amna and S. M. Alhassan, *ACS Appl. Polym. Mater.*, 2024, **6**, 4350–4377.
- 27 K.-S. Kang, C. Olikagu, T. Lee, J. Bao, J. Molineux, L. N. Holmen, K. P. Martin, K.-J. Kim, K. H. Kim, J. Bang, V. K. Kumirov, R. S. Glass, R. A. Norwood, J. T. Njardarson and J. Pyun, *J. Am. Chem. Soc.*, 2022, **144**, 23044–23052.
- 28 J. Y. Chao, T. J. Yue, B. H. Ren, G. G. Gu, X. B. Lu and W. M. Ren, *Angew. Chem., Int. Ed.*, 2022, **61**, e202115950.
- 29 H. Huang, S. Zheng, J. Luo, L. Gao, Y. Fang, Z. Zhang, J. Dong and N. Hadjichristidis, *Angew. Chem., Int. Ed.*, 2024, **63**, e202318919.
- 30 T. Gleede, L. Reisman, E. Rieger, P. C. Mbarushimana, P. A. Rugar and F. R. Wurm, *Polym. Chem.*, 2019, **10**, 3257–3283.
- 31 S. Jung, S. Kang, J. Kuwabara and H. J. Yoon, *Polym. Chem.*, 2019, **10**, 4506–4512.
- 32 I. C. Stewart, C. C. Lee, R. G. Bergman and F. D. Toste, *J. Am. Chem. Soc.*, 2005, **127**, 17616–17617.
- 33 T. Homann-Müller, E. Rieger, A. Alkan and F. R. Wurm, *Polym. Chem.*, 2016, **7**, 5501–5506.
- 34 E. Rieger, T. Gleede, K. Weber, A. Manhart, M. Wagner and F. R. Wurm, *Polym. Chem.*, 2017, **8**, 2824–2832.
- 35 C. Bakkali-Hassani, C. Coutouly, T. Gleede, J. Vignolle, F. R. Wurm, S. Carlotti and D. Taton, *Macromolecules*, 2018, **51**, 2533–2541.
- 36 P. C. Mbarushimana, Q. Liang, J. M. Allred and P. A. Rugar, *Macromolecules*, 2018, **51**, 977–983.
- 37 L. Reisman, E. A. Rowe, E. M. Jackson, C. Thomas, T. Simone and P. A. Rugar, *J. Am. Chem. Soc.*, 2018, **140**, 15626–15630.
- 38 S. Kobayashi, *Prog. Polym. Sci.*, 1990, **15**, 751–823.
- 39 O. Ihata, Y. Kayaki and T. Ikariya, *Angew. Chem., Int. Ed.*, 2004, **43**, 717–719.
- 40 D. Tan, X. Hu, Z. Cao, M. Luo and D. J. Darensbourg, *ACS Macro Lett.*, 2020, **9**, 866–871.
- 41 H. Huang, H. Wei, L. Huang, T. Fan, X. Li, Z. Zhang and T. Shi, *Eur. Polym. J.*, 2023, **182**, 111731.

- 42 D. Sureshkumar, T. Gunasundari, V. Ganesh and S. Chandrasekaran, *J. Org. Chem.*, 2007, **72**, 2106–2117.
- 43 W. Chen, E. W. Rosser, D. Zhang, W. Shi, Y. Li, W.-J. Dong, H. Ma, D. Hu and M. Xian, *Org. Lett.*, 2015, **17**, 2776–2779.
- 44 A. G. Németh, R. Szabó, K. Németh, G. M. Keserű and P. Ábrányi-Balogh, *Org. Biomol. Chem.*, 2022, **20**, 4361–4368.
- 45 T. T. T. Nguyen, V. A. Le, P. Retailleau and T. B. Nguyen, *Adv. Synth. Catal.*, 2020, **362**, 160–165.
- 46 M. Guerre, C. Taplan, J. M. Winne and F. E. Du Prez, *Chem. Sci.*, 2020, **11**, 4855–4870.
- 47 J. Zheng, Z. M. Png, S. H. Ng, G. X. Tham, E. Ye, S. S. Goh, X. J. Loh and Z. Li, *Mater. Today*, 2021, **51**, 586–625.
- 48 N. J. Van Zee and R. Nicolaÿ, *Prog. Polym. Sci.*, 2020, **104**, 101233.